Bidirectional Current Conveyer with Chopper Stabilization and Dynamic Element Matching

Hamed Mazhab Jafari, Roman Genov
Department of Electrical and Computer Engineering, University of Toronto, Email: {hamed, roman}@eecg.utoronto.ca

***Abstract*—A compact and accurate current conveyer for interfacing with a three-electrode electrochemical sensor is presented. It employs chopper stabilization to reduce transistor sizes for a given flicker noise. A current-copying circuit generates a mirror image of the sensor current for bidirectional conveying. It employs dynamic element matching to remove the mismatch in the current mirrors. The current conveyer prototyped in 0.13μm CMOS consumes 4μW from a 1.2V supply. It achieves an input-referred noise of 0.13p*Arms* over a 1kHz bandwidth with a dynamic range of 8.6pA to 350nA. The prototype has been validated in DNA catalytic reporter detection.**

I. Introduction

A number of promising sensory interfaces for biological and chemical sensing applications have been introduced in recent years, such as sensory systems for monitoring of chemical neural activity of the brain [1] and for DNA detection [2-4]. Electrochemical amperometric sensing [3] is gaining popularity in such applications.

Fig. 1 shows a block diagram of an electrochemical amperometric sensing system [5]. The electrochemical cell consists of a working electrode (WE), a counter electrode (CE) and a reference electrode (RE). The transducer holds the working electrode at a known potential and records the redox current generated due to the voltage difference between the working and reference electrodes. The counter electrode provides the current required to keep the voltage difference between the working and reference electrodes constant. The reference electrode is set to a constant voltage for constant-potential amperometry (CP), a bidirectional ramp voltage for cyclic voltammetry (CV), or a small-amplitude sinusoid for impedance spectroscopy (IS).

In biochemical sensors, biologically active compounds, such as artificial antibodies, enzymes or receptors, are integrated with the working electrode. The integration process is performed by the immobilization and stabilization of biological sensor molecules on the electrode surface. For example, in DNA sensing applications the surface of the working electrode is functionalized with probe DNA. Binding of the probe DNA with the target DNA results in variation of the working electrode surface properties such as impedance or surface charge. The variation of the surface properties results in a change in the recorded value and waveform features of the redox current, thus indicating the thermodynamics and kinetics of chemical reactions at the sensory interface. In most biochemical sensing applications the recorded redox current is in the range of pA to nA and the biosensor frequency response covers a range of 1Hz to 1kHz [5].

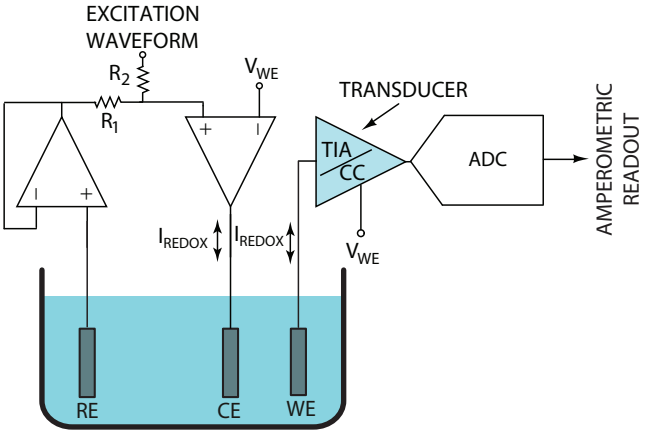

Fig. 1. Conceptual view of a three-electrode amperometric sensory system.

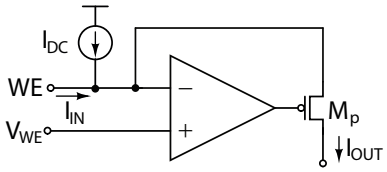

Fig. 2. Conventional bidirectional current conveyer with a DC offset current.

Several integrated circuit transducer configurations exist for measuring the redox current. The use of a transimpedance amplifier is the most common approach [3]. In this approach the transimpedance amplifier (TIA) sets a virtual potential at the working electrode and at the same time generates an output voltage that is proportional to the redox current. The main drawbacks of this method are injection of the switching noise into the sensor working electrode in case of a switched-capacitor implementation, or addition of thermal noise in the case of a resistive feedback configuration. The switching and thermal noise injected into the working electrode may alter the charge at the working electrode, thus degrading the electrochemical recording results accuracy.

Using a current conveyer (CC) is another common method of measuring the redox current [6]. In this method, the WE is held at a virtual potential. Instead of converting the redox current directly to voltage, it is conveyed from WE to a high-impedance node and then can be converted to a voltage. The advantage of this method, compared to a transimpedance amplifier, is that the working electrode is isolated from the clocked circuitry (e.g, ADC, comparator) thus reducing the

978-1-4673-0219-7/12/$31.00 ©2012 IEEE

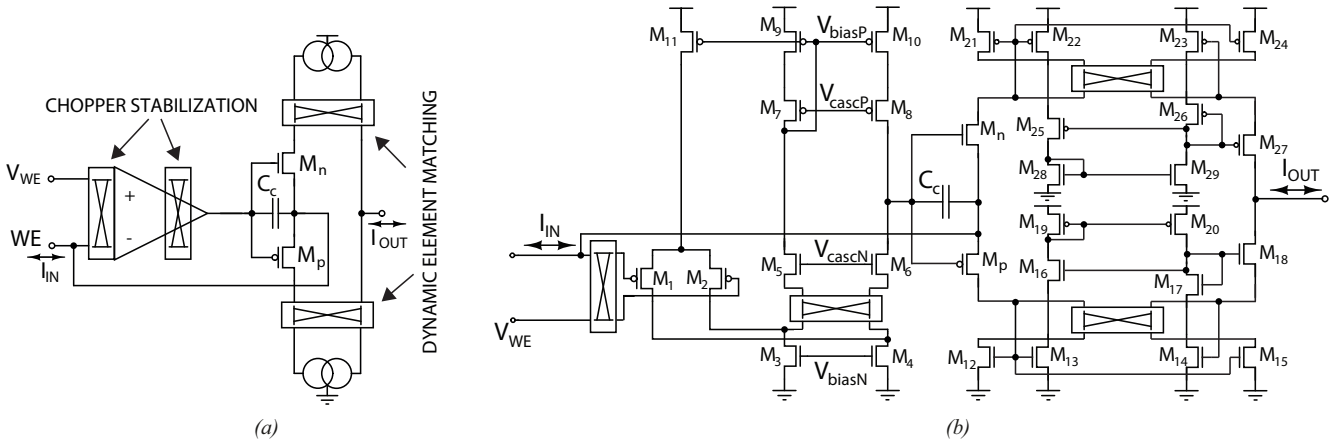

Fig. 3. (a) Bidirectional current conveyer VLSI architecture, and (b) its circuit schematic diagram.

effect of charge injection into the working electrode due to high-frequency switching. A number of current conveyer designs for electrochemical sensing applications have been reported [6-10]. In general, these designs do not support bidirectional current recording and suffer from the amplifier flicker noise and the mismatch within current mirrors.

Most electrochemical biosensing applications require sourcing and sinking the redox current. One common method to record a bidirectional current is to use a unidirectional current conveyer and to add a DC offset current to its input as shown in Fig. 2 [7]. This requires high resolution in the subsequent ADC and adds noise to the redox current. Also, depending on the WE impedance, a portion of the DC offset current can leak into the electrochemical cell and disturb the charge balance on the WE-electrolyte interface.

We present a low-noise and accurate current conveyer for biochemical sensing applications. Internal OTA chopper stabilization is utilized to reduce the effect of flicker noise. The current conveyer utilizes low-current regulated cascode current mirrors to record low bidirectional currents. Dynamic element matching is utilized to improve the accuracy by averaging the mismatch in the current mirrors. It achieves a dynamic range of 8.6pA to 350nA. The complete electrochemical recording system consists of a three-electrode regulation loop and an on-chip dual-slope ADC for digitizing the output of the current conveyer.

II. VLSI ARCHITECTURE

The top-level VLSI architecture of the bidirectional current conveyer is shown in Fig. 3(a). It is comprised of a PMOS and an NMOS transistors M_n and M_p connected in the feedback of the OTA. The negative feedback ensures a known potential at the working electrode is set by the voltage at the non-inverting input of the OTA. It also enables the current conveyer to source and sink input current without the need for a DC offset current. The currents through M_n and M_p are mirrored to the output of the current conveyer.

Internal OTA chopping has been utilized to reduce the effect of its flicker noise. The current mirrors are implemented in a low-current regulated cascode topology to enable accurate current copying down to the pA level. The current mirrors are dynamically matched to reduce the effect of their mismatch.

TABLE I
CURRENT CONVEYER TRANSISTOR SIZING

Transistor	W/L (μm)	Transistor	W/L (μm)
$M_{1,2}$	$8 \times 3/0.4$	$M_{16,17,18}$	$1 \times 0.5/4$
$M_{3,4}$	$1 \times 0.5/5$	$M_{19,20}$	$8 \times 0.3/5$
$M_{5,6}$	$4 \times 0.5/4$	$M_{21,22,23,24}$	$2 \times 0.4/8$
$M_{7,8}$	$8 \times 0.5/4$	$M_{25,26,27}$	$4 \times 0.7/3$
$M_{9,10}$	$2 \times 0.5/0.5$	$M_{28,29}$	$4 \times 0.3/4$
M_{11}	$4 \times 1/4$	M_p	$1 \times 1/1$
$M_{12,13,14,15}$	$1 \times 0.4/8$	M_n	$1 \times 0.4/4$

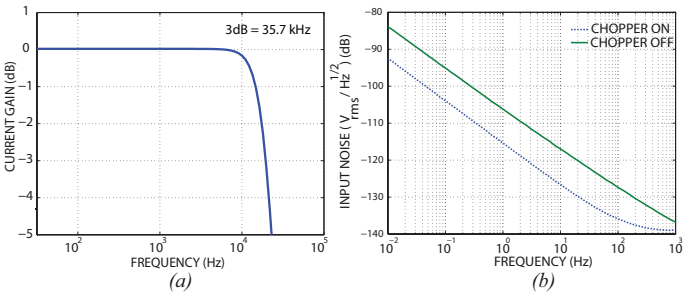

Fig. 4. (a) Simulated current conveyer AC response, and (b) Simulated input referred noise spectrum of the current conveyer from 0.01Hz to 1kHz.

III. CIRCUIT IMPLEMENTATION

The schematic diagram of the current conveyer is shown in Fig. 3(b). The OTA is implemented as a folded-cascode amplifier and the current mirrors are implemented as a low-current regulated cascode current mirror comprised of the transistors M_{12} to M_{20} and M_{21} to M_{29} [11]. The regulated cascode current mirrors ensure high precision and high output impedance of the current conveyer. The regulated current mirrors monitor I_{IN} (through M_{13} and M_{22}) and adjust the gate voltage of M_{18} and M_{27} such that the drain-source

TABLE II
CURRENT CONVEYOR NOISE SUMMARY

Transistor	Noise Source	Total Noise Chopper OFF	Total Noise Chopper ON
$M_{3,4}$	Flicker	39.12%	10.10%
$M_{1,2}$	Flicker	18.3%	7. 5%
M_{12}	Flicker	11.9%	19.8%
M_{21}	Flicker	11.5%	19.3%
M_{24}	Flicker	6.25%	17.20%
M_{15}	Flicker	6.22%	17.02%
$M_{3,4}$	Thermal	1.26%	1.96%
$M_{1,2}$	Thermal	1.2%	1.88%
M_{12}	Thermal	1.02%	1.49%
M_{21}	Thermal	0.8%	1.1%

voltage of M_{12}-M_{15} pair and M_{21}-M_{24} pair are equal thus ensuring accurate current copying down to pA level.

In this design, internal OTA chopping has been implemented to reduce the effect of both flicker noise and the input offset voltage. As shown in Fig. 3 (b), chopper switches are placed at the input of the OTA. Another set is placed after the NMOS tail current source. This significantly reduces the flicker noise and offsets due to the input pair transistors and the NMOS tail current source transistors. Minimum size switches are utilized to reduce the effect of charge injection into the working electrode. The current conveyer transistor sizes are shown in Table I.

In typical electrochemical sensing applications, the current conveyer operates in the frequency range of 0.01Hz to 1kHz. To achieve efficient flicker noise reduction, the chopper frequency needs to be higher than the input signal frequency. The chopper clock frequency was set to 10kHz. As a result the current conveyer bandwidth should be higher compared to the case where no chopper stabilization is utilized. Simulated bandwidth of the current conveyer is shown in Fig. 4(a). The current conveyer achieves a 3dB bandwidth of 35.7kHz.

The simulated input-referred noise of the current conveyer for the cases where the chopper is disabled and enabled is shown in Fig. 4(b). The integrated-input referred noise from 0.01Hz to 1kHz is 0.27pA for the case when the chopper is disabled and is 0.13pA when the chopper is enabled.

Contribution of each transistor to the total input-referred noise is shown Table II. When the chopper is disabled the main contributions are from the OTA current mirror transistors $M_{3,4}$ and the input pair transistors $M_{1,2}$. When the chopper is enabled, the current mirror transistors $M_{12,21,24,15}$ are the main contributors to the input-referred noise.

Mismatch in the regulated cascode current sources can significantly reduce the linearity of the current conveyer. Dynamic element matching (DEM) is employed to reduce the effect of the mismatch in the current mirrors. The main source of mismatch in the regulated cascode current mirrors is due to the mismatch in the transistor pairs M_{12}-M_{15} and M_{21}-M_{24}. To reduce the effect of the mismatch between these transistors, the DEM technique is applied by means of the chopper switches at the drain of the current source transistors, so that the critical transistor pairs are dynamically matched. In this method, the locations of the transistors M_{12}-M_{15} and M_{21}-M_{24} are swapped periodically, at 500Hz, effectively averaging the current mirrors mismatch.

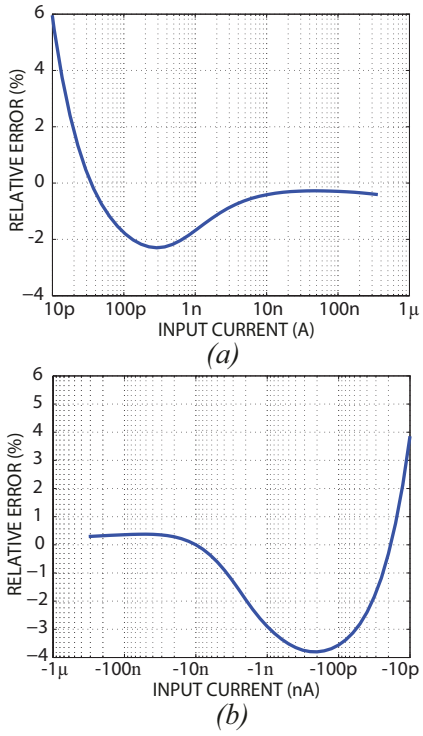

Fig. 5. Experimentally measured relative error of the output digital code of the current conveyer with a dual-slope ADC for (a) 10pA to 350nA, and (b) -350nA to -10pA.

IV. EXPERIMENTAL RESULTS

The current conveyer was fabricated in a 0.13μm CMOS process with a 1.2V supply and occupies an area of 100μm$\times$100μm. The recording channel consists of four square electrolessly plated Au WE with side length of 55μm, 5μm and 2μm sharing 250μm$\times$45μm Au RE and CE electrodes driven by an on-chip three-electrodes regulation loop.

The experimentally measured relative errors of the digital output for the input current swept between $\pm$10pA and $\pm$350nA are shown in Fig. 5. The relative error stays below 6 percent over the whole operating range. The current conveyer achieves a dynamic range of 8.6pA to 350nA. The lower limit is defined by the ADC LSB and the higher limit is defined by the input current that saturates the current conveyer.

Fig. 6 shows the experimentally recorded output current distribution for the input currents of 100pA and 100nA measured from 32 channels on 16 chips (two channels per chip) with dynamic element matching disabled and enabled. The mean output current and the corresponding standard deviation for the case when the dynamic element matching is disabled are 81.26pA and 20.2pA, respectively, for the input current of 100pA. They are 100.26nA and 34.0pA for input current of

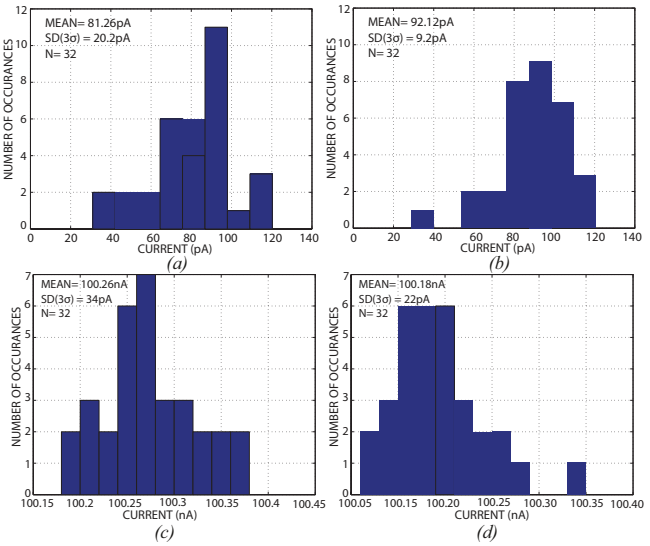

Fig. 6. Experimentally measured output current of 32 channels (from 16 chips, two channels each) for input current of (a) 100pA DEM off, (b) 100pA DEM on, (c) 100nA DEM off, and (d) 100nA DEM on.

100nA. The mean output current and standard deviation for the case when the dynamic element matching is enabled are 92.12pA and 9.2pA, respectively, for input current of 100pA. They are 100.18nA and 22.0pA, respectively, for the input current of 100nA.

To validate the performance of the current conveyer in electrochemical sensing applications, CV scans of a DNA reporter have been performed. Potassium ferricyanide $K_3[Fe(CN)_6]$ is commonly used in electrochemical DNA detection systems as a redox reporter. Cyclic voltammetry recordings of 2μM potassium ferricyanide in 1M potassium phosphate buffer (pH 7.3) have been carried out. A 100mV/sec 0.7V peak-to-peak CV waveform with 50ms resting period was applied between the (55μm$\times 50\mu$m) WEs and an off-chip Ag-AgCl reference electrode. The resulting CV curve recorded by the chopper-stabilized channel with DEM is shown in Fig. 7. The CV curve shows two distinctive peaks at the reduction and oxidization voltages of potassium ferricyanide. Table III summarizes the experimentally measured characteristics of the current conveyer.

V. Conclusions

A low-noise chopper-stabilized current conveyer for electrochemical sensing applications is presented. A dynamically matched current copying circuit generates an accurate mirror image of the sensor current in order to accept small bidirectional input currents. The current conveyer is implemented in 0.13μm CMOS and consumes 4μW from a 1.2V supply.

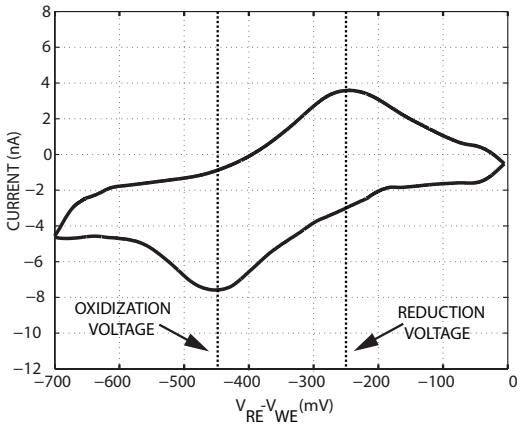

Fig. 7. Experimentally recorded cyclic voltammogram of 2μM potassium ferricyanide in 1M potassium phosphate buffer solution.

TABLE III
Experimentally Measured Characteristics

Technology	0.13μm CMOS
Supply Voltage	1.2V
Current Conveyer Area	100μm$\times 100\mu$m
Sensitivity	8.6pA
Input referred noise (0.01Hz to 1kHz)	0.13pA
Power Consumption	
Current conveyer	2μW
Biasing	1μW
Digital	1μW
Total	4μW

References

[1] M. Roham, M. P. Garris, and P. Mohseni, "A Wireless IC for Time-Share Chemical and Electrical Neural Recording," *IEEE J. Solid-State Circuits*, pp. 3645 - 3658 ,2009.

[2] F. Heer, M. Keller, G. Yu, J. Janata, M. Josowicz, A. Hierlemann, "CMOS Electro-Chemical DNA-Detection Array with On-Chip ADC," *IEEE Int. Solid-State Circuits Conf. (ISSCC)*, pp. 168-169, 2008.

[3] P. M. Levine, P. Gong, R. Levicky, K.L. Shepard, "Active CMOS Sensor Array for Electrochemical Biomolecular Detection," *IEEE J. Solid-State Circuits,* vol. 43, no. 8, pp. 1859-1871, 2008.

[4] A. Hassibi and T. H. Lee, "A Programmable 0.18μm CMOS Electrochemical Sensor Microarray for Bimolecular Detection," *IEEE Sensors Journal*, vol. 6, pp. 1380-1388, 2006.

[5] R. F. B. Turner, D. J. Harrison, and H. P. Baltes, "A CMOS Potentiostat for Amperometric Chemical Sensors," *IEEE J. Solid-State Circuits,* vol. 22, pp. 473-478, 1987.

[6] M. Nazari, H. M. Jafari, R. Genov, "192-Channel CMOS Neurochemical Microarray," *IEEE Custom Integrated Circuits Conference (CICC)*, pp. 121-125, Sept. 2010.

[7]H. S. Narula, J. G. Harris, "A Time-Based VLSI Potentiostat for Ion Current Measurement," *IEEE Sensors Journal*, vol. 6, pp. 239-247, 2006.

[8] M. Ahmadi and G. Jullien, "Current-Mirror-Based Potentiostats for Three-Electrode Amperometric Electrochemical Sensors," *IEEE Transactions on Circuits and Systems I,* vol. 56, pp. 1339-1348, 2009.

[9] S. Hwang and S. Sonkusale, "CMOS VLSI Potentiostat for Portable Environmental Sensing Applications," *IEEE Sensors Journal*, vol. 10, pp. 820-821, 2010.

[10] S. Ayers, K. D. Gillis, M. Lindau and B. A. Minch, "Design of a CMOS Potentiostat Circuit for Electrochemical Detector Arrays," *IEEE Transactions on Circuits and Systems I,* vol. **54**, no. 4, pp. 736-744, April 2007.

[11] A. Zeki and H. Kuntman, "Accurate and High Output Impedance Current Mirror Suitable for CMOS Current Output Stages," *IEEE Sensors Journal*, vol. 6, pp. 1380-1388, 2006.